Nigerian Journal of Engineering, Vol. 30, No. 2, August 2023, ISSN (print): 0794 – 4756, ISSN(online):2705-3954.

Nigerian Journal of Engineering,
Faculty of Engineering, Ahmadu Bello University, Zaria, Nigeria
journal homepage: www.njeabu.com.ng

The Effect of Magnetic Flux Density Magnitude on Machine Performance

C. C. Awah*
Department of Electrical and Electronic Engineering, Michael Okpara University of Agriculture, Umudike, PMB 7267, Umuahia, Abia State, Nigeria
* awahchukwuemeka@gmail.com

Research Article

Abstract

The effect of magnetic flux density magnitude on electromagnetic performance of a double stator permanent magnet synchronous machine is investigated and presented in this study. Finite element analysis method is applied in computing the results. The considered machine variables are: torque, losses, efficiency and electromagnetic power. The results reveal that output performances of a given machine would be affected by the magnitude of its magnetic flux density, particularly under saturation condition. Most promising electric machine characteristics are shown to be obtained from the device when the magnetic flux density magnitude is within 1.5 to 2.0 Tesla. The impact of this flux density amplitude should be taken into consideration during the design and operation of electrical machines, for effective and efficient output delivery. Highest amount of output torque, power and efficiency of 2.61 Nm, 109.46 W and 89.22 % are obtained from the simulated model at flux density amplitude of 1.6 Tesla.

doi: 10.5455/nje.2023.30.02.05

Keywords
Efficiency, magnet flux density, torque, power and saturation.

Article History
Received: – April, 2023
Reviewed: – June, 2023
Accepted: – July, 2023
Published: – August, 2023

1. Introduction

Magnetic flux density is an essential parameter which influences the overall output of any given electrical machine. Therefore, detailed analysis of the effects of this vital parameter on the output of an electric machine is presented in this present study. The analysis is intended to provide appropriate guide on implementation of magnetic flux density magnitude, for optimal electromagnetic performance. Moreover, electrical machine that exhibits negligible reluctance torque components, such as the understudied machine in this current investigation, would generally have a linear relationship between its magnetic flux density amplitude and its resulting output torque (McFarland *et al*, 2015). Nevertheless, very large amount of magnetic flux density in a given electric machine would result to high core loss magnitude; regardless of its other excellent potentials, such as high electromagnetic torque (Tsunata *et al*, 2021).

Double airgap machines would usually generate higher magnetic flux density value than its corresponding single airgap machines (Kim and Lipo, 2016). Note that the investigated machine in this current study has double airgap structure; basically, for better output performance. The resulting amount of airgap flux density of a machine would greatly affect its torque, loss and efficiency values, as demonstrated in (Wang and Jing, 2022). Nevertheless, the grade of the implemented permanent magnet (PM) material would determine its resultant flux density magnitude. It is proved that neodymium magnets have improved magnetic flux density value than its corresponding samarium-cobalt counterparts (Ozmen and Onat, 2021); and consequently, exhibits better electrical efficiency.

The amount of magnetic flux density in an electrical machine is vital in predicting its output performances (Pan and Jing, 2021); hence, a dual airgap machine having better magnetic flux density and Halbach array magnet arrangement is proposed in Pan and Jing, (2021), for enhanced machine mechanical strength as well as better output performance. The adoption of Halbach array magnet techniques in enhancing machine output is re-emphasized in (Huang *et al*, 2021); though, substantial influence of magnetic flux density magnitude is a function of its useful harmonic elements. The statement about the great importance of working magnetic flux density harmonic elements is proved in Lin *et al*, (2023), where the active magnetic flux density harmonics are prevalent in a machine's torque production.

Pham and Foster, (2020) noted that proper management of the relative permeability of adopted magnetic materials through suitable industrial procedures, could help in improving the machine's magnetic flux density worth, for better-quality overall performance. However, implementation of improved magnetic materials in electrical machines is very essential for enhanced performances (Palangar and Soong, 2022). Also, the impact of eccentricity in a rotating electrical machine would critically influence its output features (Wang and Wang, 2023).

Evans *et al*, (2010) noted that the size of PM materials of an electrical machine would be comparative to its resulting magnetic flux density magnitude, within normal operating limits of the machine i.e. prior to saturation period of the

device. Therefore, optimal magnet thickness or size is suggested in order to realize the most competitive output from a given electric machine. It is proved in Qi *et al*, (2023) that electric loading of a given electric machine would distort both its magnetic flux density amplitude as well as its resultant waveforms, owing to the adverse properties of armature reaction. Magnetic Saturation can occur in electrical machine owing to the following: its core material composition, due to its armature windings or and the excitation sources, such as permanent magnets. However, the level of electromagnetic saturation in such a device is commensurate with its effect on the machine's output performance (Lu *et al*, 2023). Thus, the higher the saturation level, then, the larger its impact on the electromagnetic performances, and vice-versa.

In this present investigation, effect of magnetic flux density amplitude on the electromagnetic performance of a double stator electric machine would be analyzed as a guide on appropriate application of a suitable magnetic flux density value, for optimal yield and consequently, help to prevent saturation effects of the device. The background of study is presented in Section 1 of this present investigation, while the adopted method and applied materials are provided in Section 2. The predicted results are discussed in Section 3. The conclusions are drawn accordingly in Section 4.

2. Materials and Methods

2.1 Methodology

MAXWELL-2D/ANSYS computational software is deployed in the predicted results of this study. The predictions are conducted through finite element analysis (FEA) technique, however, the predicted torque-speed and power-speed curves are further post-processed using MATLAB m-file at peak voltage and current of 22.9 V and 15 A, respectively. The implemented machine parameters and materials are given in Table 1. The considered variables are: torque, power, losses and efficiency. The predicted flux-weakening capability (k) of the analyzed machine is mathematically expressed in Eq. (1). The copper loss of the analyzed machine is calculated using Eq. (2). More so, the estimated efficiency (η) of the simulated model is provided in Eq. (3).

$$\boldsymbol{k} = {}^{\boldsymbol{LI}}/_{\Psi} \quad (1)$$

where: Ψ_m is the flux-linkage of magnet, I is the rated current and L is the d-axis inductance (Wei et al, 2017).

$$\boldsymbol{Copper\ Loss} = \mathbf{3}\, \boldsymbol{I_{rms}^2 R_a} \quad (2)$$

where: R_a is the armature phase resistance and I_{rms} is the root mean square value of the applied current.

$$\eta = \frac{\boldsymbol{Output\ Power}}{\boldsymbol{Output\ Power + Eddy\ Current\ Loss + Core\ Loss + Copperloss}} \quad (3)$$

The windage and friction losses are not considered in this analysis. The numerical values of

Table 1 is obtained through the inherent evolutionary optimization technique of the adopted software, as implemented in (Awah, 2022). The basic machine parameters are inputted in the Properties Section of the software. The implemented rotational speed and electric period are provided in the Motion-Setup and Analysis-Setup units of the software. A Transient Solution Type (TST) is chosen, owing to its high precision capability to predict electromagnetic fields compared to the software's Magneto-static, Eddy current, Electrostatic and Conduction Solution Modes. Additionally, discrete mesh having tiny triangular dimensions is applied, for enhanced accuracy. The model is excited with a three-phase current waveform, displaced equally in space. It is worth mentioning that the phase flux linkage, induced voltage, force and electromagnetic torque waveforms and values of the simulated model is outputted as computer auto-generated results, which is then applied in post-processing of other machine variables. The unit of magnetic flux density is represented as Tesla or T in this investigation.

Table 1 Machine parameters

Parameter/unit	value
Number of rotor pole	11
Number of slots/stator	6
Machine axial length (mm)	25
Machine outer radius (mm)	45
Winding factor	0.6
Type of magnet	neodymium-iron-boron
Magnet relative permeability	1.05
Stator resistance (Ω)	0.0493
Magnet residual flux density (Tesla)	1.2
Rotor and stator material	Silicon steel
Conductor material	Copper
Operating temperature (°C)	20
Machine split ratio	0.64
Back iron thickness (mm)	3.57
Base speed (r/min)	400
Magnet width (mm)	4.94
Rotor radial size (mm)	4.86
Shaft radius (mm)	10.4
Turns/phase	36
Number of coils/phase	2
Total number of turns/phase	72
Airgap length (mm)	0.5
Combined half-slot area (mm^2)	202.56

3. Results and Discussion

The magnetic flux lines of the simulated model on no-load condition are displayed in Figure 1. The predicted results revealed that the resulting flux lines linking the stator and rotor parts of the machine through the air-gap are proportionate to its magnetic flux density magnitudes; nevertheless, saturation effects of the armature winding could hinder the impact of these flux density magnitudes; especially, at high electromagnetic load settings.

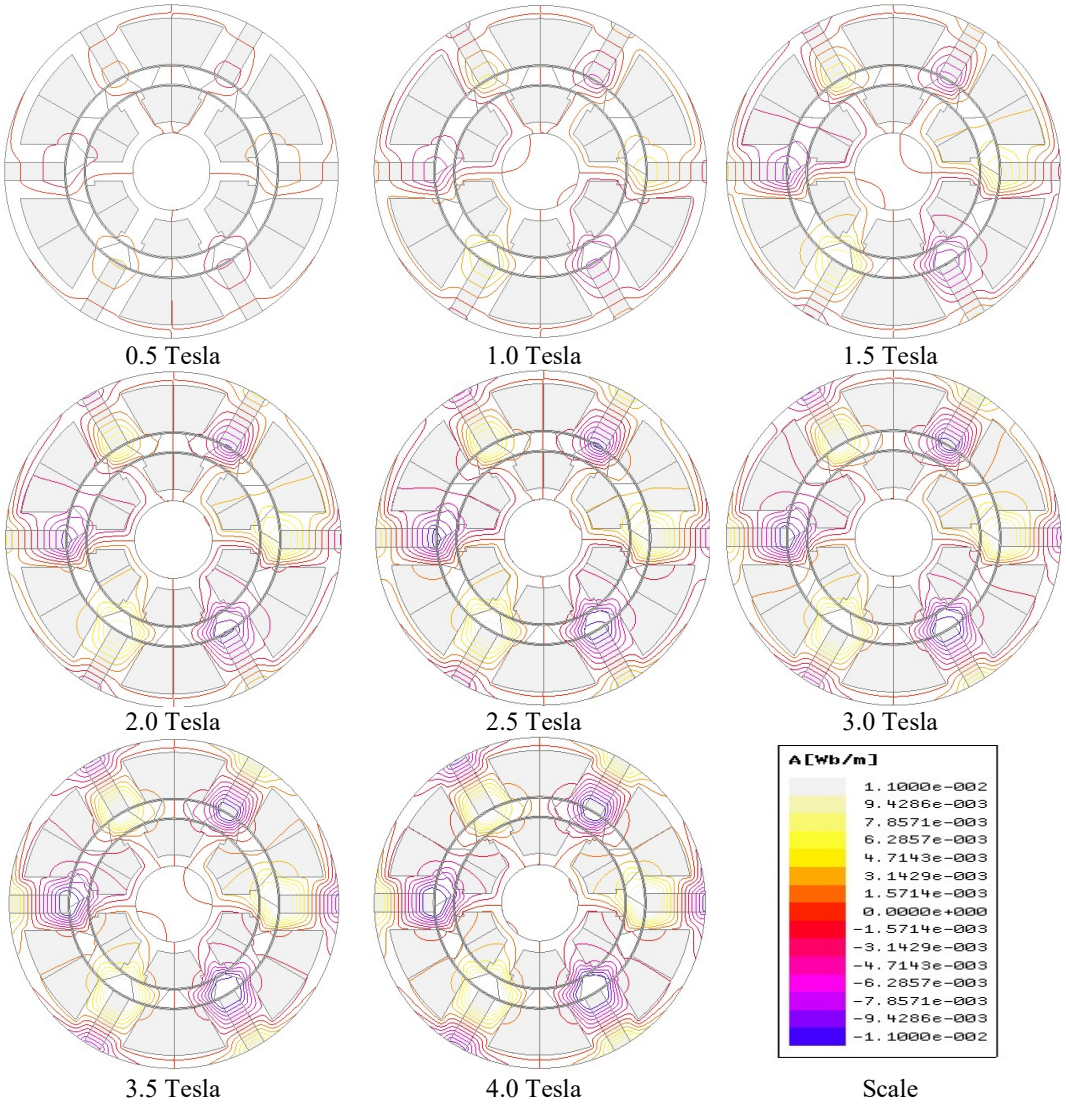

Figure 1: Magnetic flux lines on no-load

The average torque of the analyzed machine is compared in Figure 2. It is observed that average torque values tend to decrease after the 2.0 T point; regardless of the linear relation that occurred before the 2.0 T magnetic flux density value. The largest average torque of the machine is obtained at 2.0 T within the simulated current angle range, as presented in Figure 3. It is worth mentioning that the least amount of torque is obtained when magnetic flux density value of 0.5 Tesla is evaluated.

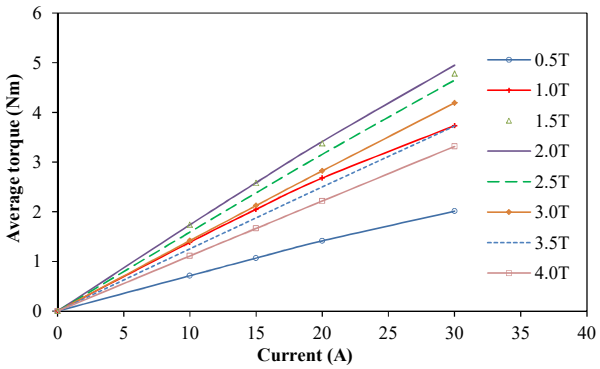

(a) Average torque versus current

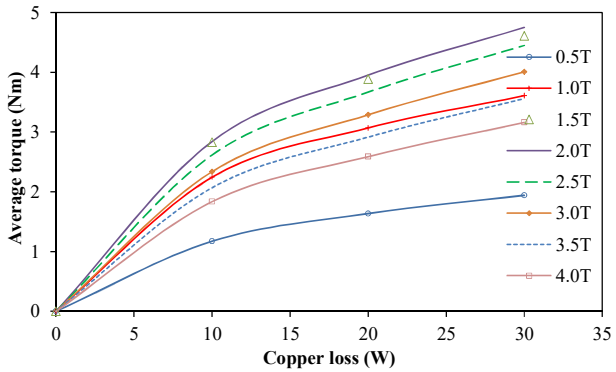

(b) Average torque versus copper loss

Figure 2 Average torque comparisons

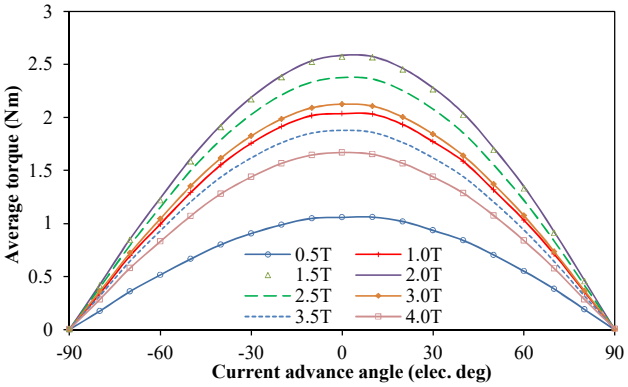

Figure 3 Average torques against current angle

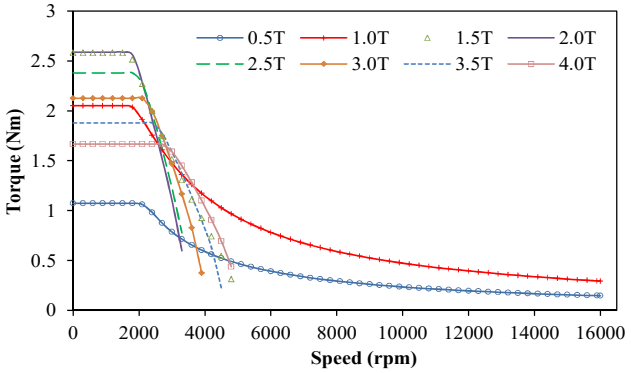

(a) Torque

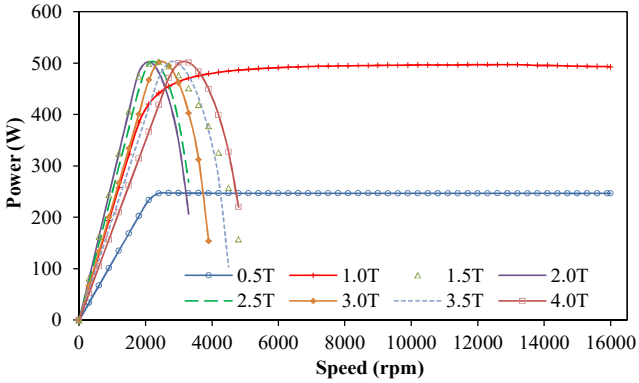

(b) Power

Figure 4 Torque speed and power speed outlines

Figure 4 shows the torque-speed and power-speed paths of the simulated model. It is revealed that extended or wider speed coverage of the analyzed machine is obtained at relatively low value of magnetic flux density. The extended speed range features of the simulated model signify its flux-weakening ability; this ability is also represented in Table 2. It is worth noting that largest electromagnetic torque and power are generated when the machine operates within 1.5 Tesla to 2.0 Tesla amplitudes, as depicted in Figure 4. However, the torque and power densities of a given electric machine could be enhanced by adopting suitable magnetic material, such as soft magnetic composite (SMC) materials (Fang *et al*, 2019) and (Chen *et al*, 2020). Nevertheless, SMC materials are usually characterized by poor manufacturing tolerance and low vector magnetization quality (Guo *et al*, 2023).

The predicted eddy current loss and core loss values given in Figure 5(a) and 5(b), show that an increase in magnetic flux density magnitude, would proportionately give rise to high amount of losses. It is also shown that saturation effect occurs in the device, beyond the flux density amplitude of about 1.6 Tesla, as presented in Table 2. Moreover, the decrease in loss at high flux density amplitudes could also be attributed to the inverse relation that exists between flux density amplitudes and loss coefficients, as concluded from (Biasion *et al*, 2022).

Figure 6(a) shows the comparison of resulting PM flux per pole at different magnetic flux density values. The highest PM flux value is realized within magnetic flux density range of 1.5–2.0 Tesla. Additionally, it is observed that the PM flux decreases as the electric loading increases, owing to saturation effect of the windings coupled with the impact of magnetic flux density magnitudes. The highest efficiency value of the analyzed model is achieved at a magnetic flux density value of 1.6 Tesla, as given in Table 3. Efficiency of the simulated machine could be improved, if magnet segmentation is applied; because magnet eddy current loss contributes mainly to poor efficiency of any given rotating electric machine (Ding *et al*, 2020). The analyzed machine performances are also provided in Tables 2 and 3.

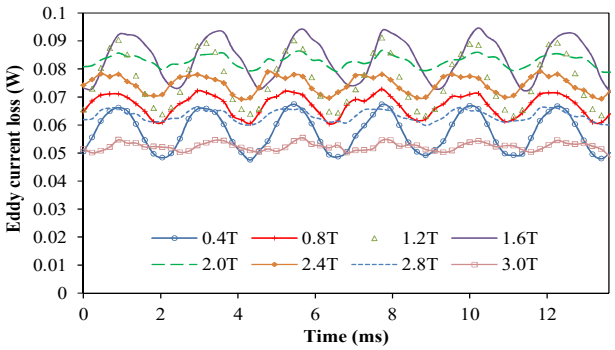

(a) Eddy current loss

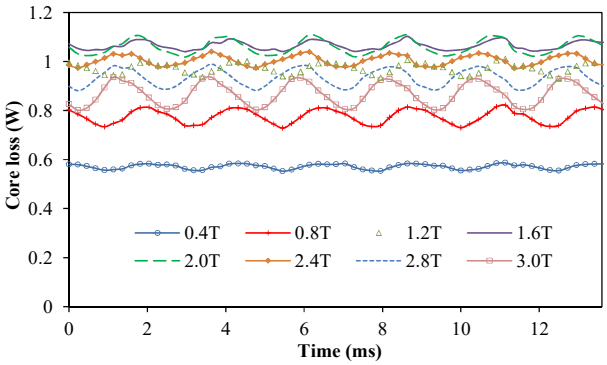

(b) Core loss

Figure 5 Loss comparisons

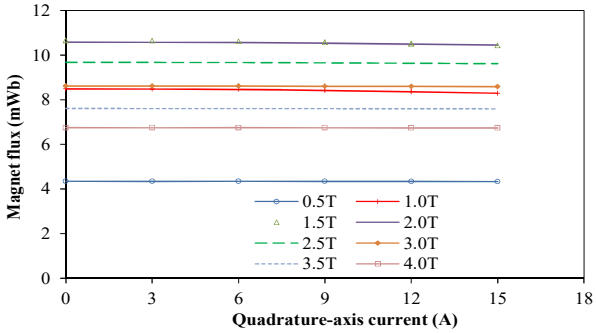

(a) PM flux

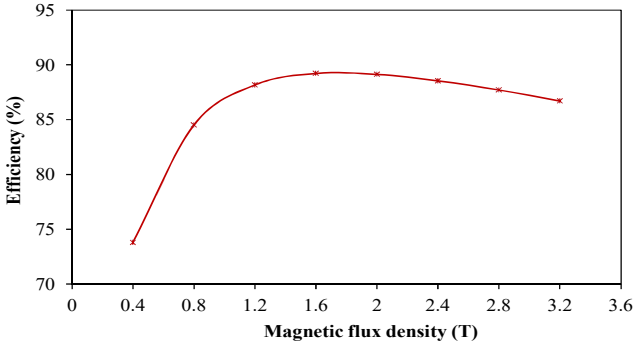

(b) Efficiency

Figure 6 Magnet flux and efficiency plots

Figure 7(a) shows that the unbalanced magnetic force (UMF) magnitude of the analyzed machine is directly proportional to the machine's magnetic flux density value. Also, the percentage of peak magnetic force on the rotor at different magnetic flux densities is shown in Figure 7(b). The predicted UMF value is: 128 N, 240 N, 332 N and 420 N at 1 T, 2 T, 3 T and 4 T, respectively.

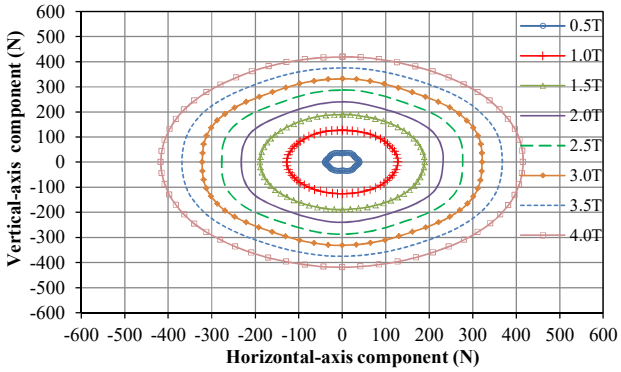

(a) Axis forces

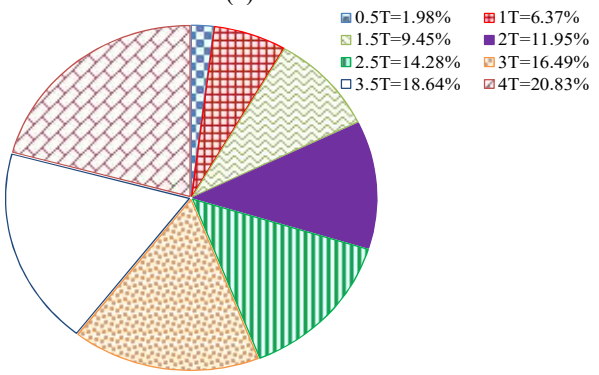

(b) Percentage of maximum force

Figure 7 Comparison of unbalanced magnetic force on the rotor

Table 2: Torque-speed performance

Magnetic flux density (T)	0.5 T	1.0 T	1.5 T	2.0 T	2.5 T	3.0 T	3.5 T	4.0 T
Maximum speed (rpm)	16000	16000	4900	3400	3500	4000	4500	5000
Base speed (rpm)	2000	1700	1700	1800	1900	2100	2400	2700
Speed ratio	8	9.41	2.88	1.94	1.84	1.9	1.88	1.85
Field weakening capability	2.0494	1.0096	0.64	0.47	0.43	0.42	0.43	0.42

Table 3: Output of the analyzed machine at 400 rpm

Magnetic flux density (T)	0.4 T	0.8 T	1.2 T	1.6 T	2.0 T	2.4 T	2.8 T	3.2 T
PM eddy current loss (W)	0.06	0.07	0.08	0.08	0.08	0.07	0.06	0.05
Core loss (W)	0.6	0.8	1	1.1	1.1	1	0.9	0.9
Torque (Nm)	0.9	1.7	2.3	2.6	2.6	2.4	2.2	2
Electromagnetic power (W)	36	71	98	109	108	102	93	85
Efficiency (%)	74	85	88	89	89	89	88	87

4. Conclusion

The impact of magnetic flux density amplitude on output performance of a given electric machine is analyzed and presented in this study. It is revealed that output performance(s) of a given electrical machine is influenced by its magnetic flux density magnitude and these performances would be negatively affected during saturation effect of the flux density. However, linear relationship is maintained between the applied magnetic flux densities and its resulting unbalanced magnetic forces. Moreover, the largest output torque, power and efficiency of the analyzed machine are obtained at magnetic flux density of about 1.6 Tesla. However, the analyzed machine would yield its optimum flux-weakening ability at relatively low magnetic flux density amplitude. This study is aimed at guiding electrical machine designers on the appropriate implementation of magnetic flux density magnitude required for effective and efficient machine output performance. The predicted results are recommended for experimental validation.

References

Awah, C.C. (2022). A new topology of double-stator permanent magnet machine equipped with AC windings on both stators, *Archives of Electrical Engineering*, Vol. 71(2), pp. 283–296.

Biasion, M., Peixoto, I.S.P., Fernandes, J.F.P., Vaschetto, S., Bramerdorfer, G., and Cavagnino, A. (2022). Iron loss characterization in laminated cores at room and liquid nitrogen temperature. 2022 *IEEE Energy Conversion and Exposition (ECCE)*, Detroit, USA, pp. 1–8.

Chen, Q., Liang, D., Jia, S., Ze, Q., and Liu, Y. (2020). Analysis of winding MMF and loss for axial flux PMSM with FSCW layout and YASA topology. *IEEE Transactions on Industry Applications*, Vol. 56(3), pp. 2622–2635.

Ding, H., Zhang, L., Hembel, A., and Sarlioglu, B. (2020). Investigation of the effects of skew of an integrated flux-switching motor-compressor. 2020 *IEEE Energy Conversion and Exposition (ECCE)*, Detroit, USA, pp. 5545–5552.

Evans, D., Azar, Z., Wu, L.J., and Zhu, Z.Q. (2010). Comparison of optimal design and performance of pm machines having non-overlapping windings and different rotor topologies. 5th *IET International Conference on Power Electronics, Machines and Drives (PEMD 2010)*, Brighton, UK. pp. 1–7.

Fang, S., Liu, H., Wang, H., Yang, H., and Lin, H. (2019). High power density PMSM with lightweight structure and high-performance soft magnetic alloy core. *IEEE Transactions on Applied Superconductivity*, Vol. 29(2), pp. 1–5.

Guo, Y., Ba, X., Liu, L., Lu, H., Lei, G., Yin, W., and Zhu, J. (2023). A review of electric motors with soft magnetic composite cores for electric drives. *Energies*, Vol. 16(4), pp. 2053.

Huang, X., Guo, Y., and Jing, L. (2021). Comparative analysis of electromagnetic performance of magnetic gear. *Progress in Electromagnetics Research Letters*, Vol. 97(3), pp. 69–76.

Kim, B., and Lipo, T.A. (2016). Analysis of a PM vernier motor with spoke structure. *IEEE Transactions on Industry Applications*, Vol. 52(1), pp. 217–225.

Lin, S., Chang, L., Su, P., Li, Y., Hua, W., and Shen, Y. (2023). Research on high-torque-density design for axial modular flux-reversal permanent magnet machine. *Energies*, Vol. 16(4), pp. 1691.

Lu, W., Zhu, J., Fang, Y., and Pfister, P.D. (2023). A hybrid analytical model for the electromagnetic analysis of surface-mounted permanent-magnet machines considering stator saturation, *Energies*, 16(3), pp. 1300.

McFarland, J.D., Jahns, T.M., and A.M. EL-Refaie. (2015). Analysis of the torque production mechanism for flux-switching permanent-magnet machines. *IEEE Transactions on Industry Applications*, Vol. 51(4), pp. 3041–3049.

Ozmen, T., and Onat, N. (2021). The effects of magnetic circuit geometry and material properties on surface mounted permanent magnet synchronous generator performance, *Balkan Journal of Electrical and Computer Engineering*, Vol. 9(2), pp. 99–105.

Palangar, M.F. and Soong, W.L. (2022). Future electrical machine materials: Possibilities, opportunities and challenges. 2022 *IEEE Energy Conversion and Exposition (ECCE)*, Detroit, USA, pp. 1–7.

Pan, Y., and Jing, L. (2021). Characteristic research on double rotor permanent magnet motor with irregular Halbach array. *Progress in Electromagnetics Research M*, 104(6), 133–144.

Pham, T.Q., and Foster, S.N. (2020). Additive manufacturing of non-homogeneous magnetic cores for electrical machines-opportunities and challenges. 2020 *International Conference on Electrical Machines (ICEM)*, Gothenburg, Sweden, pp. 1623–1629.

Qi, J., Zhu, Z.Q, Yan, L., Jewell, G.W., Gan, C., Ren, Y., Brockway, S., and Hilton, C. (2023). Influence of armature reaction on electromagnetic performance and pole shaping effect in consequent pole PM machines. *Energies*, Vol. 16(4), pp. 1982.

Tsunata, R., Takemoto, M., Ogasawara, S., and Orikawa, K. (2021).Variable flux memory motor employing double-layer delta-type PM arrangement and large flux barrier for traction applications. *IEEE Transactions on Industry Applications*, Vol. 57(4), pp. 3545–3561.

Wang, J., and Wang, Y. (2023). Electromagnetic torque analysis and structure optimization of interior permanent magnet synchronous machine with air-gap eccentricity. *Energies*, Vol. 16(4), pp. 1665.

Wang, Y., and Jing, L. (2022). A new structure for the coaxial magnetic gear with HTS bulks for fitness car, *Progress in Electromagnetics Research Letters*, Vol. 103(2), pp. 39–48.

Wei, H., Zhang, H., Cheng, M., Meng, J., and Hou, C. (2017). An outer rotor flux-switching permanent magnet machine with wedge-shaped magnets for in-wheel light traction, *IEEE Transactions on Industrial Electronics*, Vol. 64(1), pp. 69–80